Environmental Science & Technology

ARTICLE

pubs.acs.org/est

Formation of Nanocolloidal Metacinnabar in Mercury-DOM-Sulfide Systems

Chase A. Gerbig,*[,‡] Christopher S. Kim,[§] John P. Stegemeier,[§] Joseph N. Ryan,[‡] and George R. Aiken[†]

[‡]Department of Civil, Environmental, and Architectural Engineering, University of Colorado, 428 UCB, Boulder, Colorado 80309, United States

[§]School of Earth and Environmental Sciences, Chapman University, One University Drive, Orange, California 92866, United States

[†]U.S. Geological Survey, 3215 Marine Street, Suite E127, Boulder, Colorado 80303, United States

Supporting Information

ABSTRACT: Direct determination of mercury (Hg) speciation in sulfide-containing environments is confounded by low mercury concentrations and poor analytical sensitivity. Here we report the results of experiments designed to assess mercury speciation at environmentally relevant ratios of mercury to dissolved organic matter (DOM) (i.e., <4 nmol Hg (mg DOM)$^{-1}$) by combining solid phase extraction using C_{18} resin with extended X-ray absorption fine structure (EXAFS) spectroscopy. Aqueous Hg(II) and a DOM isolate were equilibrated in the presence and absence of 100 μM total sulfide. In the absence of sulfide, mercury adsorption to the resin increased as the Hg:DOM ratio decreased and as the strength of Hg-DOM binding increased. EXAFS analysis indicated that in the absence of sulfide, mercury bonds with an average of 2.4 $\pm$ 0.2 sulfur atoms with a bond length typical of mercury-organic thiol ligands (2.35 Å). In the presence of sulfide, mercury showed greater affinity for the C_{18} resin, and its chromatographic behavior was independent of Hg:DOM ratio. EXAFS analysis showed mercury−sulfur bonds with a longer interatomic distance (2.51−2.53 Å) similar to the mercury−sulfur bond distance in metacinnabar (2.53 Å) regardless of the Hg:DOM ratio. For all samples containing sulfide, the sulfur coordination number was below the ideal four-coordinate structure of metacinnabar. At a low Hg:DOM ratio where strong binding DOM sites may control mercury speciation (1.9 nmol mg^{-1}) mercury was coordinated by 2.3 $\pm$ 0.2 sulfur atoms, and the coordination number rose with increasing Hg:DOM ratio. The less-than-ideal coordination numbers indicate metacinnabar-like species on the nanometer scale, and the positive correlation between Hg:DOM ratio and sulfur coordination number suggests progressively increasing particle size or crystalline order with increasing abundance of mercury with respect to DOM. In DOM-containing sulfidic systems nanocolloidal metacinnabar-like species may form, and these species need to be considered when addressing mercury biogeochemistry.

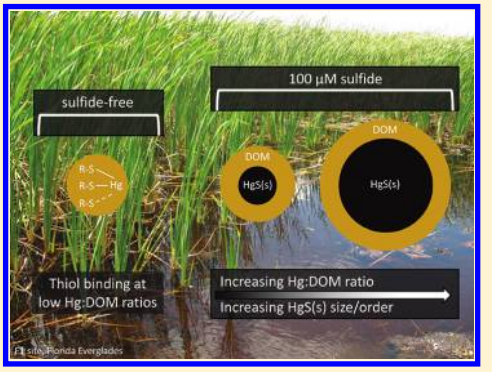

INTRODUCTION

Predicting the fate and transport of soft, chalcophilic metals in the environment depends in part on metal speciation in the presence of sulfide and dissolved organic matter (DOM). The speciation of mercury (Hg) is of particular concern because of the potential formation of methylmercury (especially in sulfate-reducing systems [1]) and bioaccumulation in aquatic food chains.[2] Studies of other metals have identified nanocolloidal metal-sulfide minerals in sulfide-containing systems, including ZnS(s) in biofilms[3] and at microbial interfaces,[4] and CuS(s) in experimentally flooded wetlands[5] and experimental systems containing DOM.[6] Colloidal mercury-sulfide minerals, particularly metacinnabar (β-HgS(s)), the low-temperature polymorph of HgS(s), have been observed in experimental systems[7−9] and at mining[10] and contaminated field sites[11] but not in natural sulfate-reducing environments with relatively low mercury concentrations and no point-source contamination.[12]

Efforts to thermodynamically model the speciation of Hg(II) primarily focus on Hg-DOM complexes in the absence of sulfide and Hg-sulfide complexes in the absence of DOM. Provided the mercury concentration is sufficiently low, DOM exhibits a high affinity for Hg(II), dominating mercury speciation in typical oxic surface waters.[13−18] The high strength of Hg-DOM interactions at low Hg:DOM ratios, coupled with directly observed mercury-soil organic matter binding sites,[19−21] suggests DOM binding sites are thiol-like in nature, although the mercury coordination environment has never been directly observed in aquatic DOM as it has been in soil organic matter. Studies of mercury speciation with sulfide in the absence of DOM show rapid precipitation of metacinnabar[22] and a number of dissolved mercury-sulfide complexes (e.g., $HgHS_2^-$, $Hg(HS)_2^0$, HgS_2^{-2}, HgS^0), of which neutrally charged complexes have been hypothesized to be the most important for methylation.[23−28]

Received: June 1, 2011
Accepted: August 31, 2011
Revised: August 23, 2011
Published: August 31, 2011

dx.doi.org/10.1021/es201837h | Environ. Sci. Technol. 2011, 45, 9180–9187

Thermodynamic models that suggest mercury-sulfide complexes dominate mercury speciation at low mercury concentrations do not compare well with empirical observations of colloidal HgS(s) stabilized by DOM in experimental systems. In sulfide- and DOM-containing systems with a mercury concentration of 50 μM, metacinnabar particles were observed as particles or aggregates of less than 100 nm in diameter. At 50 nM Hg, the particles or aggregates, if present, were too small to remove via conventional centrifugation.[7] Similar work using ultracentrifugation has demonstrated removal of mercury particles from solutions with concentrations as low as 1 nM Hg, although the removed mercury was only definitely characterized as metacinnabar-like at 10 μM Hg.[8] The metacinnabar particles formed in the presence of DOM, sulfide, and relatively high concentrations of total mercury (i.e., >10 μM) become coated with DOM, which increases electrostatic repulsion and prevents aggregation and bulk precipitation of metacinnabar.[7−9] The direct observation of DOM-stabilized metacinnabar particles is limited to studies conducted at mercury concentrations far in excess of most natural systems, where only the weakest DOM binding sites are relevant for mercury speciation.[13] Speciation calculations, however, suggest that DOM-stabilized HgS(s) may also be present at common environmental levels of mercury, DOM, and sulfide.[9]

The goal of this study was to empirically determine mercury speciation in DOM-containing solutions with and without free aqueous sulfide at Hg:DOM ratios and total mercury concentrations that are lower than previously studied and span a range of Hg-DOM binding strengths. We adopted a solid phase extraction (SPE) method previously used to determine Hg-DOM binding constants to concentrate hydrophobic mercury species[18,29] and applied this method over a wide range of Hg:DOM ratios. The speciation of mercury concentrated by SPE was subsequently examined with extended X-ray absorption fine structure (EXAFS) spectroscopy for samples of selected Hg:DOM ratios. The results presented in this paper provide direct insight into the nature of the Hg-DOM bond and on the role of DOM in mercury speciation in sulfidic environments.

METHODS

DOM Isolation. Whole water was collected from the F1 site (26°21′35″N, 80°22′14″W) in the Florida Everglades, filtered through a 0.3 μm glass fiber filter, acidified to pH 2 with HCl, and passed through a column of Amberlite XAD-8 resin according to the method of Aiken et al.[30] The hydrophobic acid fraction (HPoA; comprised of humic and fulvic acids) was retained on the XAD-8 resin and eluted with 0.1 N NaOH. The eluate was hydrogen-saturated, desalted, freeze-dried, and stored for later use. This DOM isolate has been used in several studies of mercury-organic matter interactions.[7,13,14,31] Information on the DOM source and characterization is available elsewhere.[12,32]

Experimental Solutions. Two identical sets of experimental solutions were prepared − a set for experiments only involving SPE and a set for SPE followed by EXAFS analysis of mercury on the resin. Experimental solutions for both sets were prepared in deionized water (≥18.0 MΩ cm resistivity) and contained 0.01 M NaH_2PO_4, enough $NaClO_4$ to bring the ionic strength to 0.1 M (as calculated by Visual MINTEQ[33]) and an appropriate amount of 0.1 M NaOH to bring the pH to 6.5 ± 0.1. DOM stock solution was prepared daily, filtered (0.45 μm Supor membranes), and added to the experimental solutions to yield a DOM concentration of approximately 10 mg L^{-1} for all SPE and most SPE-EXAFS experiments (measured range 8.6−11.3 mg DOM L^{-1}). Some of the SPE-EXAFS experiments were conducted at approximately 50 mg DOM L^{-1}. Appropriate volumes of Hg(II) stock solution ($Hg(NO_3)_2$ in 10% HNO_3) were spiked into the experimental solutions to achieve mercury concentrations ranging from 0.35 nM to 1.4 μM. The range of mercury and DOM concentrations allowed some experiments to be conducted at a Hg:DOM ratio at or below 4 nmol Hg (mg DOM)$^{-1}$, the ratio at which all strong binding DOM sites become saturated and weak-binding sites begin to also bind mercury.[13] Sulfide-containing solutions were prepared in an oxygen-free glovebox. Sodium sulfide ($Na_2S \cdot 9H_2O$; washed before use) stock solution was prepared daily and added to experimental solutions to bring the total sulfide concentration to 100 μM. Solution bottles were wrapped with aluminum foil to prevent photoreactions and allowed to mix at room temperature on a shaker table rotating at 150 rpm. Solutions were equilibrated for 20−24 h, which has been shown elsewhere to give sufficient time for Hg-DOM equilibration[34,35] and Hg-DOM-sulfide equilibration.[9,36] Containers for solution/stock preparation and sampling were glass with Teflon-lined caps cleaned in a solution of 10% HNO_3 and 10% HCl (trace metal-grade) for at least 24 h and baked at 400 °C for 4 h.

Solid Phase Extraction. The SPE portion of the experiments was carried out on glass columns (10 cm length, 0.9 cm diameter; Spectrum Chromatography) packed with 0.500 g of C_{18} resin (Supelclean ENVI-18, Spectrapor). The column fittings and lines were Teflon, except for the pump tubing, which was polyvinylchloride. Resin-free columns and tubing were cleaned with a mixture of 10% HNO_3 and 10% HCl and rinsed repeatedly with deionized water. Clean resin was prepared in the column by suspending resin in methanol and rinsing (20 min per rinse at 4 mL min^{-1}) with deionized water followed by 5 mM HCl, repeating once, and concluding with deionized water. The loss of mercury to a resin-free column (<5%) and contamination from a resin-filled column (<0.03 nM) were sufficiently small to be ignored in the subsequent SPE experiments, but there was some DOC contamination from resin-filled columns (<5 mg C L^{-1}; presumably methanol).

Cleaned and resin-filled columns were loaded with approximately 1 L of experimental solution for SPE experiments and 2 L of solution for SPE-EXAFS experiments. Experimental solutions were pumped through the cleaned resin-filled columns at a flow rate of 4.0 ± 0.2 mL min^{-1}. After expunging the first 2 mL of solution out of each column, the remaining loaded volume was collected as effluent fractions for chemical analyses. Resin was harvested from the column following solution loading and was stored under an oxygen-free atmosphere for sulfide-containing experiments until EXAFS analysis. Mercury recovery from the SPE experiments, including mercury in effluent fractions and mercury adsorbed to the resin, was greater than 90% of the total mercury loaded. Error in the SPE of mercury was related to errors in mercury measurements (described in next section) and depended on the amount of mercury passing through the resin. At high retentions (>90%) the error was less than 1% retained mercury, and at lower retentions (~60%) the error was approximately 4% retained mercury.

Sample Analysis. Dissolved organic carbon (DOC) concentrations were determined using a total organic carbon analyzer (OI Analytical Model 700). DOM concentrations were calculated based on DOC measurements and the carbon content of

the Everglades F1 HPoA isolate (52.2% C by mass). Measurements of ultraviolet and visible light absorbance at wavelengths ranging from 254 to 412 nm were made using a UV−visible spectrophotometer (Agilent model 8453) with a 1 or 5 cm path length quartz cuvette.

Total aqueous mercury concentrations in initial and effluent samples from the SPE were determined by cold vapor atomic fluorescence spectroscopy using a Millennium Merlin mercury analyzer according to EPA Method 245.7. Analytical mercury stocks were prepared from National Institute of Standards and Technology (NIST) standard reference material 3133. Mercury standards and most samples were oxidized with 1% (v/v) KBr/$KBrO_3$ solution. High DOM and sulfide-containing samples were oxidized with 2% (v/v) KBr/$KBrO_3$ solution to ensure sufficient residual oxidant to preserve mercury after oxidation of organic matter and sulfide species. Acceptable recovery of standards was 80−120% with less than 20% relative difference in duplicate measurements. Typical recovery was 90−110% with less than 10% relative difference. The detection limit for any given run was always below 0.013 nM Hg based on three standard deviations of seven replicates of a sample with a concentration one-half of the lowest standard.

Solid phase mercury concentrations on the harvested chromatography resin were measured on a DMA-80 direct mercury analyzer (Milestone Inc.) by thermal decomposition of the sample, catalytic conversion to elemental mercury, amalgamation, and atomic absorption. Calibration was done with a series of standard reference materials obtained from NIST and Environment Canada. Acceptable recovery of the reference materials was 80−120%.

Extended X-ray Absorption Fine Structure Spectroscopy. Resin samples were prepared for EXAFS by loading 2 L of the experimental solutions outlined in SI Table 1 onto C_{18} resin. Two liters of solution were necessary to maximize the amount of mercury loaded onto the resin due to the relatively high concentration threshold (approximately 40 ppm Hg) needed to collect viable EXAFS spectra. The top third of the resin in the column was removed from the column and used for EXAFS analysis because solid phase mercury analysis indicated it was more concentrated than the resin in the bottom two-thirds of the column.

EXAFS data were collected on wiggler beamline 11−2 at the Stanford Synchrotron Radiation Lightsource using a Si(220) monochromator crystal in the φ = 90° crystal orientation. Mercury L_{III}-edge EXAFS spectra were collected using an aluminum coldfinger liquid nitrogen cryostat (77 K) to minimize thermal vibration and improve the quality of the spectra from low mercury concentration samples. The resin samples were loaded into aluminum holders in an oxygen-free environment, enclosed in Kapton tape, and quickly transferred to the liquid nitrogen cryostat to minimize exposure to oxygen. Spectra were collected on a 32-element high-throughput germanium detector in fluorescence-yield mode. Gallium filters were used to minimize interference from inelastic scattering. $HgCl_2$ was used as an internal standard for energy calibration of each spectrum collected.

Multiple scans (13−22) were collected for each sample, energy-corrected using the calibration standard, deadtime-corrected for potential loss of signal due to finite photon detection times, and averaged together. After background subtraction, the data were converted to k-space with a k^3-weighting and Fourier-transformed. The EXAFS spectra were fit over a k-range of 2.0−9.5 $Å^{-1}$ using phase and amplitude functions from model single-shell scattering paths generated in SIXPack[37] using Feff6l.[38] Hg−C, Hg−O, and Hg−S models (the only realistic first shell interactions in Hg-DOM-sulfide systems) were created and constrained based on the results of the first shell fitting of the resin samples. Mixed interactions were attempted (i.e., Hg−O and Hg−S), but single atom interactions consistently proved to be better fits. Given the limited energy range over which spectra were resolvable, only first shell fitting was successfully completed for each resin sample. The scale factor (S_0) was fixed at 0.9 for all samples, and the Debye−Waller factor (σ^2), which serves as a measure of thermal vibration and static disorder around mercury in the sample, was first allowed to float for all fits; the average Debye−Waller factor for all samples (0.007 $Å^2$) was selected and final fits fixed at this value in order to directly compare fitting results between samples.

RESULTS

DOM Solid Phase Extraction. The absorption of ultraviolet and visible (UV−vis) light was used to track DOM adsorption to the C_{18} resin because small amounts of methanol contamination in effluent fractions led to erratic DOC measurements. DOM retention by the resin was consistent regardless of mercury concentration (0.35 nM−1.4 μM) or the presence or absence of sulfide (Figure 1a). DOM retention decreased as the volume of loaded solution increased (SI Figure 1). The fraction of UV−vis-absorbing components retained by the resin increased with increasing wavelength but was generally low − less than 35%. The UV−vis absorbance of DOM at 254 nm correlates well with the aromaticity of the organic matter,[39] although more conjugated molecules are expected to absorb at 412 nm. These data indicate that the more conjugated organic molecules are also somewhat more hydrophobic and preferentially adsorb to the resin.

Mercury Solid Phase Extraction. Retention of mercury by C_{18} resin was a function of mercury concentration and the presence or absence of sulfide (Figure 1b), unlike the retention of DOM. Mercury adsorption to the column did not change substantially through the course of loading up to 1 L of sulfide-free solution (SI Figure 2). The overall efficiency of mercury adsorption from sulfide-free solutions was dependent on the mercury concentration in the loading solution (Figure 1b). At 5.6 nM Hg and below, the retention of mercury was 85−91%. At 39 nM Hg and above, retention dropped to 48−61%.

Retention curves for mercury in systems containing 100 μM total sulfide were distinctly different from those without sulfide (SI Figure 2). The retention of mercury from a sulfide-containing solution with 0.45 nM Hg increased as the total volume loaded increased. In contrast, at mercury concentrations from 1.5 to 490 nM, the mercury adsorption was consistently high (Figure 1b, SI Figure 2). Based on these chromatography results, the mercury species formed in the presence of sulfide at higher mercury concentrations are slightly more hydrophobic (>99% retention at 490 nM) than those formed at lower mercury concentrations (95% retention at 1.5 nM) and substantially more hydrophobic than those formed in the absence of sulfide. For all cases, greater than 60% of the mercury retained by the resin was present in the top one-third of the column based on solid phase analysis.

The 0.45 nM Hg and sulfide solution resulted in uncommon chromatographic behavior − the retention of mercury increased as the volume of solution loaded onto the resin increased. Such behavior indicates that the sorbent phase becomes more favorable for the sorption of the compound in solution as the amount

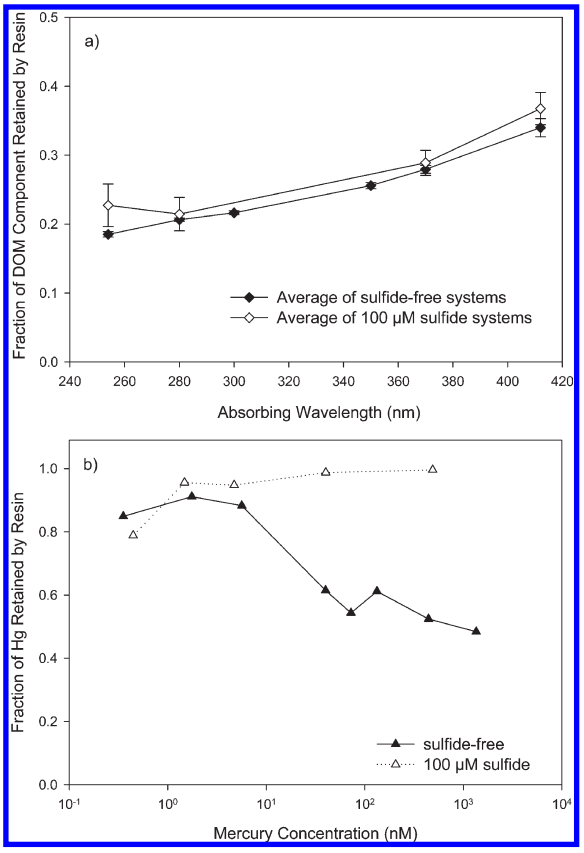

Figure 1. (a) The average fraction of ultraviolet and visible light-absorbing DOM components retained by the C_{18} resin as a function of absorbing wavelength for approximately 1 L of eight sulfide-free and five sulfide-containing solutions. Error bars represent 95% confidence intervals for all mercury concentrations. (b) The fraction of total mercury retained on C_{18} resin for all experiments with DOM (8.6−11.3 mg DOM L^{-1}) and with and without sulfide as a function of total mercury concentration.

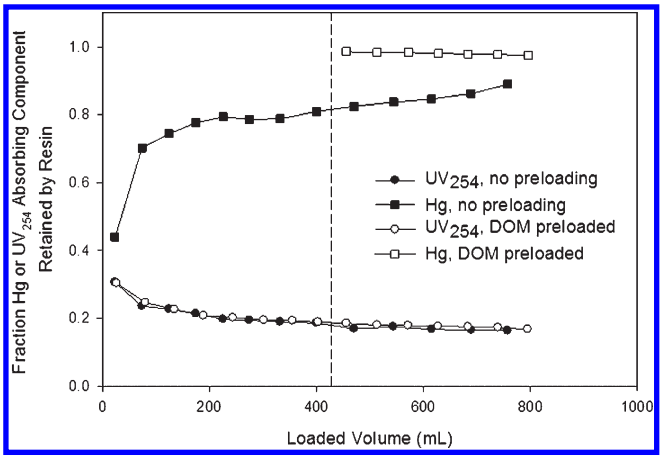

Figure 2. Mercury retention and DOM retention (as measured by the UV absorbance of DOM components that absorb at 254 nm) for a system without DOM preloading of the resin and a system with DOM preloading of the resin. The system without preloading (0.45 nM Hg, 10.6 mg DOM L^{-1}, 100 μM sulfide) was run as a standard chromatography experiment with the mercury-containing solution started at a loaded volume of 0 mL. The preloaded system consisted of DOM preloading (9.8 mg DOM L^{-1}, 100 μM sulfide) up to a volume of 428 mL (dashed vertical line) at which time an identical solution equilibrated with mercury (0.40 nM) was loaded on to the resin.

of the sorbed compound increases. In the mercury-DOM-sulfide systems in this study, two components are accumulating on the resin—mercury and DOM—and either could be responsible for the increased retention of mercury with loaded volume. Either the adsorption of mercury from solution could promote the sorption of more mercury, which could potentially lead to the formation of mercury species on the resin which are not present in solution, or the adsorption of DOM from solution could promote the adsorption of more DOM along with the bound mercury species.

To determine which mechanism was responsible for the increasing mercury retention with increased loading, we compared the retention of mercury from the 0.45 nM Hg, 100 μM sulfide, 10.6 mg DOM L^{-1} solution with the retention of mercury after the resin was preloaded with DOM (Figure 2). A mercury-free preloading solution (9.8 mg DOM L^{-1}, 100 μM sulfide, 428 mL) was loaded onto C_{18} resin and followed with an identical solution that also contained 0.40 nM Hg. The DOM retention was identical in both systems as indicated by the retention of UV_{254} absorbing components (Figure 2). After preloading the resin with DOM, mercury retention was initially very high (>97%), and the retention did not increase with increased loading volume as observed in the system without preloading. We interpret the difference in mercury retention to mean that mercury−mercury interactions were not driving mercury retention because the DOM-preloaded system showed high mercury retention at the beginning of mercury loading. Had mercury retention increased with volume after DOM preloading, there would have been evidence for mercury−mercury interactions, which would have brought into question whether the mercury species on the resin are present in solution. Instead, we surmise that DOM served as a bridge between the mercury species in solution and the resin, and an abundance of DOM on the resin increased mercury affinity for the sorbent phase.

Extended X-ray Absorption Fine Structure Spectroscopy. Experimental and fitted mercury L_{III}-edge EXAFS spectra and the Fourier transforms corresponding to the conditions outlined in SI Table 1 are shown in Figure 3. The EXAFS spectra of the three sulfide-containing systems (Figure 3b, 3c, and 3d) are in phase with one another and out of phase with the sulfide-free sample (Figure 3a). This corresponds with the alignment of the primary Fourier transform features of the sulfide-containing samples (indicated in Figure 3 by a vertical line) and the misalignment of the sulfide-containing samples with the sulfide-free sample. The spectra for samples with added sulfide (3b, 3c, and 3d) were best modeled by a mercury−sulfur bond in the first shell with a Hg−S interatomic distance of 2.51−2.53 Å (±0.01−0.02 Å, depending on the sample; Figure 3). The mean sulfur coordination number for the sulfide-containing samples increased with increasing Hg:DOM ratio from 2.3 ± 0.2 sulfur atoms at 1.6 nmol Hg (mg DOM)$^{-1}$ to 3.3 ± 0.2 sulfur atoms at 34 nmol Hg (mg DOM)$^{-1}$. The spectra for the sample without added sulfide (3a) was also best modeled by mercury−sulfur bonds in the first shell, despite the absence of added sulfide in the sulfide-free system. The Hg-DOM interaction was fit with a significantly shorter Hg−S distance of 2.35 ± 0.01 Å and a coordination number of 2.4 ± 0.2 sulfur atoms.

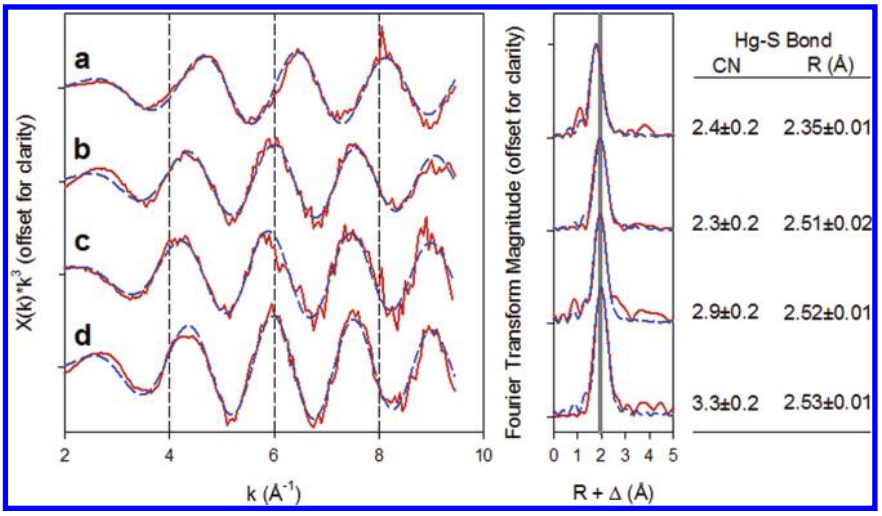

Figure 3. k^3-weighted mercury L_{III}-edge EXAFS, Fourier transforms, and fitting results for collected spectra (solid) and fits (dashed) for the four SPE-EXAFS samples: (a) sulfide-free at a Hg:DOM ratio of 4.0 nmol Hg (mg DOM)$^{-1}$; (b, c, and d) 100 μM total sulfide and Hg:DOM ratios of 1.9, 4.9, and 34 nmol Hg (mg DOM)$^{-1}$, respectively. Solution chemistries are summarized in SI Table 1. All spectra are best fit by a Hg−S interaction. The sulfur coordination number (CN) and average bond distance (R) are noted for each sample with the 95% confidence interval ($\pm 2\sigma$). The Debye−Waller factor (σ^2) was fixed at 0.007 Å^2 for all four fits.

DISCUSSION

Mercury-Dissolved Organic Matter Interactions. In the absence of sulfide and at sufficiently low Hg:DOM ratios, we hypothesized that Hg-DOM binding would be dominated by mercury−sulfur interactions because (1) Hg-DOM binding studies have measured large stability constants consistent with thiol-like sites[13,15] and (2) Hg-soil organic matter (SOM) studies using EXAFS spectroscopy have detected Hg−S bonds at low Hg:SOM ratios.[20,40] We observed 2.4 coordinating sulfur atoms at 2.35 Å, which is consistent with observations of a 2−3 sulfur coordination environment in soil organic matter and soil humic acid as detected by X-ray spectroscopy[21,40] and pH titrations.[19] The Hg−S interatomic distance is in good agreement with two-coordinate mercury binding environments observed for model thiolates[41] and represents the first known direct observation of mercury binding environments in aquatic DOM. Sulfur is a relatively minor element in DOM (1.7 wt % in the isolate used in this study), and the proportion of sulfur that is actually involved in metal binding is low (<2% of the total sulfur in this isolate based on 2.4 atoms/site and a binding capacity of 4 nmol (mg DOM)$^{-1}$). Multiple sulfur atoms per site suggests the possibility that these sites may be (1) of biological origin (e.g., dithiols in protein residues), (2) the result of abiotic sulfide incorporation into DOM, or (3) the result of multiple DOM molecules coordinating a mercury atom.

The concentration requirement, or detection limit, of EXAFS restricted identification of the Hg-DOM binding environment to a Hg:DOM ratio of 4.0 nmol Hg (mg DOM)$^{-1}$, which is the strong binding capacity of the DOM isolate.[13] Hg:DOM ratios in most environmental settings are typically a few orders of magnitude lower than this strong binding capacity. The chromatographic data suggest we can extrapolate information gained at the Hg:DOM ratio of 4.0 nmol Hg (mg DOM)$^{-1}$ to lower and more environmentally relevant Hg:DOM ratios. The sulfide-free data in Figure 1b show high retention of mercury (>85%) at mercury concentrations below 5.6 nM Hg and lower retention of mercury (<62%) at mercury concentrations above 39 nM Hg. When normalized to the DOM content of each system (all had approximately 10 mg DOM L^{-1}), the transition observed between 5.6 and 39 nM Hg corresponds to a transition between 0.67 and 4.6 nmol Hg (mg DOM)$^{-1}$. Below the 4 nmol Hg (mg DOM)$^{-1}$ strong binding capacity of the DOM, the Hg-DOM complexes are significantly more hydrophobic with respect to the C_{18} resin than they are above the strong binding capacity. The transition from more to less hydrophobic complexes as the Hg:DOM ratio increases past 4 nmol Hg (mg DOM)$^{-1}$ corresponds to the transition from thiol-like Hg-DOM binding strengths to carboxyl-like Hg-DOM binding strengths.[13] Both types of complexes are significantly more hydrophobic than the mercury-free DOM, which is only retained at about 20% as measured by the retention of UV_{254} absorbing components (Figure 1a). The sulfur dominated binding environment observed with EXAFS at 4 nmol Hg (mg DOM)$^{-1}$ is likely only present in a small subset of DOM molecules and that subset is more hydrophobic than other portions of the DOM pool. The chromatography data shown in Figure 1b, coupled with our understanding of DOM binding strengths, suggests that the small number of DOM molecules involved in the directly observed sulfur dominated mercury binding at 4 nmol (mg DOM)$^{-1}$ persist at lower, more environmentally significant Hg:DOM ratios where EXAFS was not possible.

Mercury-Dissolved Organic Matter-Sulfide Interactions. The EXAFS spectra from all three sulfide-containing samples were best fit with a Hg−S scattering interaction at an interatomic distance of 2.51−2.53 Å (Figure 3). The Hg−S interatomic distance from all three samples agrees, within uncertainty, with the 2.53 Å Hg−S distance in crystalline metacinnabar.[22] The observed EXAFS spectra are not consistent with cinnabar (which has six coordinating sulfur atoms at three distinct distances[22]), polymeric HgS species that exhibit two sulfur atoms at a shorter distance of 2.30 Å,[26] neutrally charged complexes (i.e., HgS(aq) and HgHSOH(aq)) with a single Hg−S interaction at less than 2.40 Å,[24] nor the Hg-DOM interaction described previously. In addition, simultaneous fits of a Hg−S scattering path at 2.53 Å indicative of metacinnabar and a Hg−S scattering path at 2.35 Å

indicative of Hg-DOM complexes showed no significant DOM binding in systems that contained sulfide.

The Hg−S bond distance is independent of Hg:DOM ratio for the three sulfide-containing samples and matches well with metacinnabar, but the sulfur coordination numbers are all lower than the four-coordinate structure of crystalline metacinnabar. The modeled coordination numbers may be explained by imperfectly ordered crystal structures or nanosized HgS(s) particles where under-coordinated mercury atoms on the particle surface comprise a large percentage of all mercury atoms in the phase. The disorder in the particles may even be greater than the coordination number implies because the Debye−Waller factor was fixed in the EXAFS modeling, which implicitly assumes that changes in the spectra were related to changes in coordination number and not the degree of disorder. The modeled coordination number increases with increasing Hg:DOM ratio (Figure 3, samples b, c, and d), which suggests that the Hg:DOM ratio is an important factor in dictating the size or crystalline order of the metacinnabar-like species. Metacinnabar-like species formed at the lowest Hg:DOM ratio resemble the initial phases of metacinnabar crystallization characterized by under-coordinated mercury atoms, whereas the metacinnabar-like species formed at the highest Hg:DOM ratio resembles a structure approaching that of bulk crystalline metacinnabar.[22] The interaction of DOM with particle surfaces and subsequent control of particle aggregation has been documented for HgS(s)[7−9] and other metal sulfides and metal oxides (e.g., refs 6 and 42), although the formation of HgS(s) has never been directly observed at the mercury concentrations and Hg:DOM ratios at which mercury is interacting with the strongest DOM binding sites. The strong DOM binding sites are not strong enough to prevent the formation of metacinnabar, but the metacinnabar that forms when mercury speciation is dominated by thiol sites is smaller or less ordered than metacinnabar formed at higher Hg:DOM ratios.

Our results show that the portion of DOM interacting with the surface of HgS(s) and preventing growth is more hydrophobic with respect to fractionation on C_{18} resin than the DOM that remains in solution. The majority of the DOM in our SPE experiments passed through the column, although the portions of the DOM that absorb light at higher wavelengths, which presumably represents greater conjugation, are retained on the resin to a greater degree than the bulk DOM (Figure 1). Additionally, the hydrophobic fraction retained by the resin favors adsorption of metacinnabar-like mercury species (Figure 2). These results are supported by previously observed preferential adsorption of aromatic DOM molecules to colloidal metacinnabar particles.[7]

EXAFS-derived coordination numbers can be used to estimate particle sizes when they are significantly lower than the coordination number of the bulk phase and the particles are well ordered.[43,44] The less-than-ideal sulfur coordination numbers for the three metacinnabar-like samples observed in this study indicate the particles are on the nanometer scale. Referred to as the termination effect, this phenomenon arises when under-coordinated atoms on a particle surface make up a significant fraction of the atoms in the particle. The abundance of under-coordinated atoms drives down the average coordination number for particles in the diameter range of tens of nanometers or less. If we assume that the HgS(s) is perfectly crystalline, the less-than-ideal coordination numbers of the mercury−sulfur bonding observed in this study point to particles that are less than 20 nm in diameter, with the smallest (and most under-coordinated) particles as small as just a few nanometers in diameter. In a previous study designed to assess the importance of DOM in inhibiting the precipitation of metacinnabar,[7] metacinnabar colloids decreased in sized with decreasing mercury concentration. The minimum mercury concentration for direct characterization, 50 μM, led to metacinnabar particles or aggregates less than 100 nm as determined by centrifugation. We have now identified evidence for smaller metacinnabar-like nanoparticles at 50 nM Hg. Our results are also consistent with observations at 10 μM Hg of poorly crystalline and under-coordinated HgS(s) particles that are on the nanometer scale.[8]

The results presented here contrast with the conclusions of octanol−water partitioning studies which suggest neutrally charged species (e.g., HgS^0 and $Hg(SH)_2$) dominate mercury speciation in the presence of sulfide in natural environments.[23] DOM significantly alters the octanol partitioning of Hg−S species when mercury concentrations are as low as 0.1 nM,[36] and the partitioning of amorphous metacinnabar-like nanoparticles to octanol has been demonstrated at a mercury concentration of 3 μM.[9] Our study bridges the concentration divide by empirically observing a metacinnabar-like species at an intermediate mercury concentration, which chromatography suggests is present at even lower mercury concentrations than could be directly observed with EXAFS. Mercury-sulfide speciation modeling predicts metacinnabar will form at the intermediate and high mercury concentrations used in this study. However, the speciation modeling is ambiguous at the low concentrations in this study below about 4 nM Hg because on the uncertainty in thermodynamic constants (constants for the modeling reproduced in SI Table 2). If metacinnabar is not formed below 4 nM, then speciation modeling predicts hydrophilic complexes (primarily $HgHS_2^-$) will dominate in these systems (quantitative speciation presented in SI Figure 3). Hydrophilic complexes will not be retained by the C_{18} resin. Our data show the mercury species in sulfidic systems are consistently retained at high levels by the resin, which indicates that the HgS(s) observed at higher mercury concentrations also dominates at lower, more environmentally relevant concentrations. Modeling efforts elsewhere have shown that uncertainty in thermodynamic constants, particularly the metacinnabar solubility product, makes mercury speciation difficult to predict at environmentally relevant concentrations.[9] Our results provide empirical evidence that a discrete inorganic metacinnabar-like phase is stabilized by dissolved organic matter at mercury concentrations and Hg:DOM ratios that are more representative of natural systems.

Environmental Implications. Conventional filtration methods are insufficient to diagnose the presence or absence of nanosized particles in the environment; however, the potential exists to use a chromatographic approach to detect the presence of mercury-containing nanoparticles. Hsu-Kim and Sedlak[45] noted the adsorption of mercury species to C_{18} resin when a wastewater effluent sample was exposed to sulfide. As that study and another[9] have noted, some of those mercury species are not labile to a strong competing ligand, such as glutathione, whereas dissolved complexes with organic matter are labile. Now that direct observation of mercury speciation has identified metacinnabar (or at least, a metacinnabar-like phase) as a potential source of that nonlabile portion at lower mercury concentrations approaching environmentally relevant concentrations, the potential exists to identify similar species in natural anoxic waters with a chromatographic approach.

Knowledge of the speciation of mercury is paramount in assessing the extent and kinetics of the biologically driven conversion of

mercury into methylmercury. While this study does not attempt to determine the role of speciation in methylation, it provides evidence that sulfate-reducing microbes, which typically reside in sulfide- and organic matter-rich environments, are likely to be exposed to disordered, nanoparticulate metacinnabar stabilized by dissolved organic matter. Our results are consistent with the observation of poorly crystalline, nanometer-scale HgS(s) particles in a mercury contaminated site[11] and illuminate the role of DOM in HgS(s) formation and stabilization. The mechanism of that stabilization, the rate of nanoparticle growth and aggregation, and the role DOM-coated nanoparticulate metacinnabar plays in methylation are critical areas for further research. In addition, the thermodynamics of a nanoparticulate phase are not necessarily well represented by thermodynamic constants of the bulk phase,[46] and thus mercury speciation models may need to account for disordered nanoparticulate HgS(s).

■ ASSOCIATED CONTENT

Supporting Information. Table of the solution composition for the EXAFS samples, a table of thermodynamic constants used to calculate possible mercury speciation, a figure of typical SPE data for DOC and UV−vis-absorbing components, a figure of typical mercury SPE, and a figure of modeled mercury speciation. This material is available free of charge via the Internet at http://pubs.acs.org.

■ AUTHOR INFORMATION

Corresponding Author
*Phone: (585) 704-8167. E-mail: chase.gerbig@colorado.edu.

■ ACKNOWLEDGMENT

We thank J. Moreau for his assistance securing X-ray spectroscopy beamtime. We also thank H. Hsu-Kim at Duke University and B. McCleskey at the U.S. Geological Survey for their critical reviews of the manuscript. This research was supported by the National Science Foundation, grant #EAR-0447386, and the U.S. Geological Survey's Priority Ecosystem Science Program. Portions of this research were carried out at the Stanford Synchrotron Radiation Lightsource, a Directorate of SLAC National Accelerator Laboratory and an Office of Science User Facility operated for the U.S. Department of Energy Office of Science by Stanford University. The use of trade names in this report is for identification purposes only and does not constitute endorsement by the U.S. Geological Survey.

■ REFERENCES

(1) Compeau, G. C.; Bartha, R. Sulfate-reducing bacteria - principal methylators of mercury in anoxic estuarine sediment. *Appl. Environ. Microbiol.* **1985**, *50* (2), 498–502.

(2) Benoit, J. M.; Gilmour, C. C.; Heyes, A.; Mason, R. P.; Miller, C. L., Geochemical and biological controls over methylmercury production and degradation in aquatic ecosystems. In *Biogeochemistry of Environmentally Important Trace Elements, ACS Symposium Series v. 835*, Cai, Y., Braids, O. C., Eds.; American Chemical Society: WA, 2003; Vol. 835, pp 262−297.

(3) Labrenz, M.; Druschel, G. K.; Thomsen-Ebert, T.; Gilbert, B.; Welch, S. A.; Kemner, K. M.; Logan, G. A.; Summons, R. E.; Stasio, G. D.; Bond, P. L.; Lai, B.; Kelly, S. D.; Banfield, J. F. Formation of sphalerite (ZnS) deposits in natural biofilms of sulfate-reducing bacteria. *Science* **2000**, *290* (5497), 1744–1747.

(4) Moreau, J. W.; Weber, P. K.; Martin, M. C.; Gilbert, B.; Hutcheon, I. D.; Banfield, J. F. Extracellular proteins limit the dispersal of biogenic nanoparticles. *Science* **2007**, *316* (5831), 1600–1603.

(5) Weber, F. A.; Voegelin, A.; Kaegi, R.; Kretzschmar, R. Contaminant mobilization by metallic copper and metal sulphide colloids in flooded soil. *Nat. Geosci.* **2009**, *2* (4), 267–271.

(6) Horzempa, L. M.; Helz, G. R. Controls on the stability of sulfide sols: Colloidal covellite as an example. *Geochim. Cosmochim. Acta* **1979**, *43* (10), 1645–1650.

(7) Ravichandran, M.; Aiken, G. R.; Ryan, J. N.; Reddy, M. M. Inhibition of precipitation and aggregation of metacinnabar (mercuric sulfide) by dissolved organic matter isolated from the Florida Everglades. *Environ. Sci. Technol.* **1999**, *33* (9), 1418–1423.

(8) Slowey, A. J. Rate of formation and dissolution of mercury sulfide nanoparticles: The dual role of natural organic matter. *Geochim. Cosmochim. Acta* **2010**, *74* (16), 4693–4708.

(9) Deonarine, A.; Hsu-Kim, H. Precipitation of mercuric sulfide nanoparticles in NOM-containing water: Implications for the natural environment. *Environ. Sci. Technol.* **2009**, *43* (7), 2368–2373.

(10) Slowey, A. J.; Johnson, S. B.; Rytuba, J. J.; Brown, G. E. Role of organic acids in promoting colloidal transport of mercury from mine tailings. *Environ. Sci. Technol.* **2005**, *39* (20), 7869–7874.

(11) Barnett, M. O.; Harris, L. A.; Turner, R. R.; Stevenson, R. J.; Henson, T. J.; Melton, R. C.; Hoffman, D. P. Formation of mercuric sulfide in soil. *Environ. Sci. Technol.* **1997**, *31* (11), 3037–3043.

(12) Gilmour, C. C.; Riedel, G. S.; Ederington, M. C.; Bell, J. T.; Benoit, J. M.; Gill, G. A.; Stordal, M. C. Methylmercury concentrations and production rates across a trophic gradient in the northern Everglades. *Biogeochemistry* **1998**, *40* (2−3), 327–345.

(13) Haitzer, M.; Aiken, G. R.; Ryan, J. N. Binding of mercury(II) to dissolved organic matter: The role of the mercury-to-DOM concentration ratio. *Environ. Sci. Technol.* **2002**, *36* (16), 3564–3570.

(14) Haitzer, M.; Aiken, G. R.; Ryan, J. N. Binding of mercury(II) to aquatic humic substances: Influence of pH and source of humic substances. *Environ. Sci. Technol.* **2003**, *37* (11), 2436–2441.

(15) Lamborg, C. H.; Tseng, C. M.; Fitzgerald, W. F.; Balcom, P. H.; Hammerschmidt, C. R. Determination of the mercury complexation characteristics of dissolved organic matter in natural waters with "reducible Hg" titrations. *Environ. Sci. Technol.* **2003**, *37* (15), 3316–3322.

(16) Benoit, J. M.; Mason, R. P.; Gilmour, C. C.; Aiken, G. R. Constants for mercury binding by dissolved organic matter isolates from the Florida Everglades. *Geochim. Cosmochim. Acta* **2001**, *65* (24), 4445–4451.

(17) Han, S. H.; Gill, G. A. Determination of mercury complexation in coastal and estuarine waters using competitive ligand exchange method. *Environ. Sci. Technol.* **2005**, *39* (17), 6607–6615.

(18) Hsu, H.; Sedlak, D. L. Strong Hg(II) complexation in municipal wastewater effluent and surface waters. *Environ. Sci. Technol.* **2003**, *37* (12), 2743–2749.

(19) Khwaja, A. R.; Bloom, P. R.; Brezonik, P. L. Binding constants of divalent mercury (Hg^{2+}) in soil humic acids and soil organic matter. *Environ. Sci. Technol.* **2006**, *40* (3), 844–849.

(20) Skyllberg, U.; Xia, K.; Bloom, P. R.; Nater, E. A.; Bleam, W. F. Binding of mercury(II) to reduced sulfur in soil organic matter along upland-peat soil transects. *J. Environ. Qual.* **2000**, *29* (3), 855–865.

(21) Skyllberg, U.; Bloom, P. R.; Qian, J.; Lin, C. M.; Bleam, W. F. Complexation of mercury(II) in soil organic matter: EXAFS evidence for linear two-coordination with reduced sulfur groups. *Environ. Sci. Technol.* **2006**, *40* (13), 4174–4180.

(22) Charnock, J. M.; Moyes, L. N.; Pattrick, R. A. D.; Mosselmans, J. F. W.; Vaughan, D. J.; Livens, F. R. The structural evolution of mercury sulfide precipitate: an XAS and XRD study. *Am. Mineral.* **2003**, *88* (8−9), 1197–1203.

(23) Benoit, J. M.; Mason, R. P.; Gilmour, C. C. Estimation of mercury-sulfide speciation in sediment pore waters using octanol-water partitioning and implications for availability to methylating bacteria. *Environ. Toxicol. Chem.* **1999**, *18* (10), 2138–2141.

(24) Tossell, J. A. Calculation of the structures, stabilities, and properties of mercury sulfide species in aqueous solution. *J. Phys. Chem. A* **2001**, *105* (5), 935–941.

(25) Paquette, K. E.; Helz, G. R. Inorganic speciation of mercury in sulfidic waters: The importance of zero-valent sulfur. *Environ. Sci. Technol.* **1997**, *31* (7), 2148–2153.

(26) Bell, A. M. T.; Charnock, J. M.; Helz, G. R.; Lennie, A. R.; Livens, F. R.; Mosselmans, J. F. W.; Pattrick, R. A. D.; Vaughan, D. J. Evidence for dissolved polymeric mercury(II)-sulfur complexes? *Chem. Geol.* **2007**, *243* (1−2), 122–127.

(27) Lennie, A. R.; Charnock, J. M.; Pattrick, R. A. D. Structure of mercury(II)-sulfur complexes by EXAFS spectroscopic measurements. *Chem. Geol.* **2003**, *199* (3−4), 199–207.

(28) Benoit, J. M.; Gilmour, C. C.; Mason, R. P.; Heyes, A. Sulfide controls on mercury speciation and bioavailability to methylating bacteria in sediment pore waters. *Environ. Sci. Technol.* **1999**, *33* (6), 951–957.

(29) Black, F. J.; Bruland, K. W.; Flegal, A. R. Competing ligand exchange-solid phase extraction method for the determination of the complexation of dissolved inorganic mercury(II) in natural waters. *Anal. Chim. Acta* **2007**, *598* (2), 318–333.

(30) Aiken, G. R.; McKnight, D. M.; Thorn, K. A.; Thurman, E. M. Isolation of hydrophilic organic-acids from water using nonionic macroporous resins. *Org. Geochem.* **1992**, *18* (4), 567–573.

(31) Waples, J. S.; Nagy, K. L.; Aiken, G. R.; Ryan, J. N. Dissolution of cinnabar (HgS) in the presence of natural organic matter. *Geochim. Cosmochim. Acta* **2005**, *69* (6), 1575–1588.

(32) Ravichandran, M.; Aiken, G. R.; Reddy, M. M.; Ryan, J. N. Enhanced dissolution of cinnabar (mercuric sulfide) by dissolved organic matter isolated from the Florida Everglades. *Environ. Sci. Technol.* **1998**, *32* (21), 3305–3311.

(33) Gustafsson, J. P. *Visual MINTEQ*, version 3.0; Stockholm, Sweden, 2007. http://www2.lwr.kth.se/English/OurSoftware/vminteq/ (accessed March 1, 2011).

(34) Gasper, J. D.; Aiken, G. R.; Ryan, J. N. A critical review of three methods used for the measurement of mercury (Hg^{2+})-dissolved organic matter stability constants. *Appl. Geochem.* **2007**, *22* (8), 1583–1597.

(35) Miller, C. L.; Southworth, G.; Brooks, S.; Liang, L.; Gu, B. Kinetic controls on the complexation between mercury and dissolved organic matter in a contaminated environment. *Environ. Sci. Technol.* **2009**, *43* (22), 8548–8553.

(36) Miller, C. L.; Mason, R. P.; Gilmour, C. C.; Heyes, A. Influence of dissolved organic matter on the complexation of mercury under sulfidic conditions. *Environ. Toxicol. Chem.* **2007**, *26* (4), 624–633.

(37) Webb, S. M. SIXpack: a graphical user interface for XAS analysis using IFEFFIT. *Phys. Scr.* **2005**, *2005* (T115), 1011.

(38) Rehr, J. J.; Mustre de Leon, J.; Zabinsky, S. I.; Albers, R. C. Theoretical x-ray absorption fine structure standards. *J. Am. Chem. Soc.* **1991**, *113* (14), 5135–5140.

(39) Weishaar, J. L.; Aiken, G. R.; Bergamaschi, B. A.; Fram, M. S.; Fujii, R.; Mopper, K. Evaluation of specific ultraviolet absorbance as an indicator of the chemical composition and reactivity of dissolved organic carbon. *Environ. Sci. Technol.* **2003**, *37* (20), 4702–4708.

(40) Nagy, K. L; Manceau, A.; Gasper, J. D.; Ryan, J. N.; Aiken, G. R. Metallothionein-like multinuclear clusters of mercury(II) and sulfur in peat. *Environ. Sci. Technol.* **2011**.

(41) Manceau, A.; Nagy, K. L. Relationships between Hg(II)-S bond distance and Hg(II) coordination in thiolates. *Dalton Trans.* **2008**, *11*, 1421–1425.

(42) Kodama, H.; Schnitzer, M. Effect of fulvic acid on the crystallization of Fe(III) oxides. *Geoderma* **1977**, *19* (4), 279–291.

(43) Calvin, S.; Miller, M. M.; Goswami, R.; Cheng, S. F.; Mulvaney, S. P.; Whitman, L. J.; Harris, V. G. Determination of crystallite size in a magnetic nanocomposite using extended x-ray absorption fine structure. *J. Appl. Phys.* **2003**, *94* (1), 778–783.

(44) Frenkel, A. Solving the 3D structure of nanoparticles. *Z. Kristallogr.* **2007**, *222*, 605–611.

(45) Hsu-Kim, H.; Sedlak, D. L. Similarities between inorganic sulfide and the strong Hg(II) - complexing ligands in municipal wastewater effluent. *Environ. Sci. Technol.* **2005**, *39* (11), 4035–4041.

(46) Gilbert, B.; Banfield, J. F. Molecular-scale processes involving nanoparticulate minerals in biogeochemical systems. *Rev. Mineral. Geochem.* **2005**, *59* (1), 109–155.